BEAM BREAKUP IN A SUPERCONDUCTING ELECTRON ACCELERATOR*

K. Mittag, H. A. Schwettman and H. D. Schwarz

Department of Physics and High Energy Physics Laboratory

Stanford   University
Stanford, California

Introduction

Beam breakup sets an upper limit to the beam current achievable in a linear accelerator as is well known from theory and experience with both normal conducting accelerators and superconducting prototypes.[1,2,3] This paper focuses its interest on the beam breakup problems encountered in the injector system of the superconducting linear accelerator (SCA) for electrons under construction at Stanford University.[4] The design goal for this accelerator with respect to beam current is 100 µA and duty factor 1.

Cumulative Beam Breakup

The existence of cumulative beam breakup has been established in long normal conducting accelerators such as the 2-GeV Kharkov linac and the SLAC two-mile accelerator, and the subject has been treated in the literature both for normal conducting[5] and superconducting[6,7] linacs. Here we will point out the major differences between cumulative beam breakup in normal and superconducting linacs and estimate the importance of this effect for the Stanford SCA.

In both normal conducting and superconducting linacs rf deflecting modes of the accelerator structure are excited resonantly with small amplitudes by the noise modulated beam current, and the resulting field produces a transverse momentum modulation in the beam at the resonance frequency of the deflection mode. While the beam drifts towards the next structure this momentum modulation is converted into a transverse space modulation. Thus the beam can excite the corresponding deflecting mode of subsequent structures, and travelling downstream the beam diameter is exponentially amplified until it hits some aperture. In a normal conducting accelerator the frequency deviations of the corresponding deflecting modes in different structures are small compared to the bandwidth of the mode, and the amplification increases with increasing Q-values. In a superconducting accelerator, on the other hand, the frequency deviations in different structures are large compared to the bandwidth of the mode. The amplification no longer depends on the Q-values of the deflecting modes, but is determined instead by the frequency deviations in different structures.

In theoretical approaches to cumulative beam breakup the increase of the beam diameter along the length of the accelerator is described by an e-folding factor F , $\exp(F)$ being the ratio of beam diameters at the end and beginning of the accelerator. In the limit $\Delta\omega \gg \omega/Q_L$ where the difference in resonant frequency $\Delta\omega$ between any two structures is much greater than the bandwidth ω/Q_L of the deflecting mode, the usual expression for the e-folding factor[7] must be modified. Assuming that all structures are excited by the beam off resonance with the same detuning $\Delta\omega$, we obtain an upper limit for the e-folding factor which is

$$F_{max} = \left(\frac{2\pi\ \ell\ N\ I\ r/Q}{\lambda\ V'\ \Delta\omega/\omega}\right)^{1/2} . \qquad (1)$$

In this formula ℓ is the effective interaction length of one section, N is the number of sections in the accelerator, λ is the free space wavelength of the deflecting mode, I is the average beam current, V' is the voltage which the particles gain per unit length, and r/Q is the transverse shunt impedance of the deflecting mode.

Using this expression we can estimate the importance of cumulative beam breakup in the Stanford SCA. The r/Q-value is calculated to be 5 Ω/cm using as a model a chain of weakly coupled pillbox cavities excited in a pure TM_{11}-mode.[7] This value taken together with the parameters of the Stanford SCA (ℓ = 5.6 m, N = 25, $\omega/2\pi$ = 1.9 GHz, I = 100 µA, V' = 3.3 MV/m, r/Q = 5 Ω/cm, $\omega/\Delta\omega$ = 2 x 10^5) yields F_{max} = 4.1 . Cumulative beam breakup occurred at SLAC for a value of F on the order of 15, indicating an ample margin of safety for an average current of 100 µA. If the beam current in the Stanford SCA were increased to 500 µA, however, quadrupole focussing might be necessary.

Regenerative Beam Breakup

In contrast to cumulative beam breakup, regenerative beam breakup[8-13] is confined to single accelerator structures. Let us consider a breakup mode excited by noise with small amplitude in a standing wave structure. Those space harmonics of this mode with phase velocities similar to the beam velocity will produce a bunching of the beam, which depending on the mode can be either in the axial or radial direction. If the phase-slip between the center of such a bunch and the relevant space harmonics is such that the particles lose energy on the average to an electric field component of the mode, regenerative beam breakup can in principle occur. The threshold beam current for breakup, frequently called the starting current I_S , is defined by the condition that the power delivered from the beam into the field P_b is equal to the power losses of the mode in the structure, P_S . Since P_b is proportional to the beam current and independent of Q_L , and P_S is proportional to Q_L^{-1} , it follows that the starting current for breakup is inversely proportional to Q_L . Thus in a superconducting accelerator where Q-values are inherently very high the problem of regenerative beam breakup is more severe than in a normal conducting accelerator. Our concept for suppressing regenerative beam breakup in the Stanford SCA is to load down the breakup modes selectively.

Longitudinal Beam Breakup Involving the TM_{01}-Modes

Beam breakup involving the neighbor modes of the accelerator mode (TM_{01}-like modes) is important only at the low energy part of the accelerator, because axial bunching is proportional to γ^3 , $m\gamma$ being the relativistic particle mass. The magnitude of $I_S Q_L$ for the pre-accelerator of the Stanford SCA can be estimated using a result from Heller[11,12] which was obtained for zero acceleration but still taking the effect of all space harmonics of the breakup mode into consideration:

$$I_S Q_L = \left[\frac{4e\ell^2}{\pi^2 mc^2 \lambda \beta^3 \gamma^3} \sum_{m,n=-\infty}^{\infty} (\frac{Z_m}{Q}) \frac{A_n}{A_m} G(m,n) \right]^{-1} . \quad (2)$$

In this formula e is the charge of an electron $c\beta$ the particle velocity, λ the free wavelength of the mode, and ℓ the length of the structure. The space dependence of the axial electric field component E_z has been described by space harmonics as

$$E_z = \sum_{-\infty}^{\infty} A_m \cos \frac{m\pi z}{\ell} \quad , \quad (3)$$

and Z_m is the shunt impedance for the m-th space harmonic of this mode. The function $G(m,n)$ results from the phase slip $\alpha_m = m\pi - \omega\ell/\beta c$ between space harmonics and particles:

$$G(m,n) = \frac{\pi^3}{4\alpha_n^2} \left[\frac{\alpha_m + \alpha_n}{\alpha_m^2} (1 - \cos \alpha_m) - \frac{\alpha_n}{\alpha_m} \sin \alpha_m \right]. \quad (4)$$

Neglecting the effects of all but one space harmonic, and taking a set of parameters typical for the pre-accelerator of the Stanford SCA ($\omega/2\pi = 1.3$ GHz , $\ell = 240$ cm, $Z/Q = 8$ Ω/cm, average $\gamma = 10$) one obtains $I_S Q_L \gtrsim 6 \times 10^4$A.

Transverse Beam Breakup Involving the HEM_{11}-Modes

For iris-loaded structures the modes most likely to cause transverse beam breakup are the hybrid HEM_{11}-modes. There exist two branches of these HEM_{11}-modes which can be called the TM_{11}-like, and the TE_{11}-like branches, referring to the predominant character of each. Regenerative beam breakup calculations for these types of modes have been carried out using pure TM_{11}-mode fields.[8,10] The basic ideas and results of a generalized calculation[13] based on HEM_{11}-mode fields in a uniform periodic lossless iris-loaded structure of the standing wave type are given below.

One can show that the electric field in a uniform periodic iris-loaded structure can be described by an infinite sum of space harmonics $\vec{E}_n$, with each $\vec{E}_n$ satisfying Maxwell's equations.[14,15] The transverse component of the Lorentz force $\vec{F}_n$ exerted by $\vec{E}_n$ on a particle with charge q , travelling in the positive z-direction with constant velocity v_o can be written as[16]

$$\vec{F}_n = q[(1 - \frac{v_o}{v_{\varphi n}}) \vec{E}_{nt} + j \frac{v_o}{\omega} \nabla_t E_{nz}] e^{j(\omega t - k_n z)} . \quad (5)$$

Here $v_{\varphi n} = \omega/k_n$ is the phase velocity of the space harmonic and the indices t and z stand for the transverse and the axial directions. In a small signal approximation, assuming only small particle deflections, the fields near the axis can be described by the lowest order terms of a series expansion. Then the transverse equation of motion can be solved by elementary integrations, and the average power delivered from the beam into the field, P_b , is readily obtained. The calculation shows that beam breakup can occur not only for TM_{11}-like modes, but also for TE_{11}-like modes. In the latter case, under the condition $v_o > v_{\varphi n}$, the deflection of the particles due to the magnetic field dominates (see Eq. 5) and they lose energy while working against the transverse electric field.

In order to predict the starting current, one must calculate the stored energy W of the hybrid mode in the structure, and equate P_b and the power dissipated in the structure P_S using the relation $Q_L = \omega W/P_S$. This problem seems to be solvable only on a computer.[15] To obtain order of magnitude estimates, however, one can carry through this calculation for pure TM_{11}-modes[10] and TE_{11}-modes. The results are:

TM_{11}-modes:

$$I_S Q_L = \frac{\pi^2}{4} \frac{mc^2}{e} \frac{\lambda\beta\gamma}{\ell^2 r/Q} \frac{\left(\sum\limits_{m=-\infty}^{+\infty} A_m \frac{\sin\alpha_m}{\alpha_m}\right)^2}{\sum\limits_{m,n=-\infty}^{+\infty} A_n A_m \, G(m,n)} \qquad (6)$$

Here A_m is the amplitude of the m-th space harmonic.

TE_{11}-mode:

$$I_S Q_L = 30 \, c \, \epsilon_o \frac{mc^2}{e} \beta\gamma \left(\frac{D}{\lambda}\right)^2 \frac{\alpha}{1-\cos\alpha} \qquad (7)$$

For the TE_{11}-mode only the contribution of the fundamental space harmonic has been taken into account, and P_S has been calculated assuming a chain of weakly coupled cavities of diameter D excited in a pure TE_{11}-mode.

For the pre-accelerator of the Stanford SCA, taking the average energy ($\gamma = 10$) and using lower estimates for the phase slip factors we obtain for:

pure TM_{11}-modes:

$$I_S Q_L \gtrsim 7 \times 10^2 A$$

pure TE_{11}-modes:

$$I_S Q_L \gtrsim 6 \times 10^5 \, A \; .$$

The parameters assumed are $r/Q = 5 \, \Omega/cm$, $\ell = 240$ cm, $\omega/2\pi = 1.8$ GHz, for TM_{11}-modes, and $\omega/2\pi = 1.6$ GHz, D = 19 cm for TE_{11}-modes.

Passbands of the Injector Structures

The injector structures for the Stanford SCA are multiperiodic iris-loaded structures. Figure 1 is a diagram of the capture section, a 7-cell structure, and the pre-accelerator, a 23-cell structure assembled from three sub-structures, which together form the cryogenic injector. The 5 long cells in the center of every sub-structure are $\lambda/2$ in length, whereas the short cells are about $\lambda/3$ in length, λ being the free space wavelength of the accelerator mode at a frequency of 1.3 GHz. The ratio between the inner diameter of a long cell and the diameter of the iris is 2.45 , a value smaller than in conventional linear accelerators but somewhat larger than in separator structures. To determine the important passbands of the capture section and the pre-accelerator, shown in Figs. 2 and 3, we have measured the resonance frequencies and performed bead measurements for both the TM_{01}-modes and the HEM_{11}-modes. The effective wave numbers k of the various modes

are calculated from the expression $k = n\pi/\ell$. The effective length ℓ of the modes as well as the phase shift $n\pi$ of the mode over the length were obtained by analyzing the bead measurements. Also drawn are lines which have slopes equal to the electron velocities at injection and the output of each structure.

The multiperiodic character of the injector structures, the cell lengths, and the relatively large iris diameter lead to several unusual features in the passbands of the TM_{01}-modes and the HEM_{11}-modes. Consider, for example, the TM_{01}-modes in the pre-accelerator which are plotted in Fig. 3. Here, because the period of the structure is eight cells, the passband is split into eight sub-bands. As evident in Fig. 3, the effect on the HEM_{11}-modes is more profound. First, in contrast to typical $\pi/2$ or $2\pi/3$ mode structures, the lower branch of the HEM_{11} band is predominately TE_{11}-like, while the upper branch is predominately TM_{11}-like. The order in which the two branches occur is consistent with the resonant frequencies calculated for TE_{111} and TM_{110} modes in a right circular cylinder of length $\lambda/2$. Second, the modes of the TE_{11}-like branch are localized to the group of five long cells or to the group of short cells in each sub-structure. The resonant frequency of a TE_{111} mode depends on the length of the cavity. Since the frequency for a single long cell is about 1.54 GHz and the frequency for a single short cell is about 2.05 GHz, the coupling between these modes is extremely weak. Third, the TM_{11}-like branch of the HEM_{11} band is double-valued. The appearance of a double-valued passband, previously observed in separator structures,[14,17] suggests that the character of the coupling between cells changes from magnetic to electric as one moves from one end of the TM_{11}-like branch to the other, the magnitude of the coupling being relatively small near the minimum. Furthermore, the TE-admixture to the modes is quite strong here. Thus it is not totally surprising that the modes at 1.742 GHz and 1.788 GHz, near the minimum of the dispersion curve, are localized to the five long cells of each sub-structure.

Because of fabrication errors in real structure, the rotational symmetry is broken, and the HEM_{11}-modes are no longer degenerate. The splitting between the two polarizations of the HEM_{11}-modes varies between 50 kHz and 500 kHz in the structures measured.

Experimental Determination of Starting Currents

The experimental determination of starting currents for regenerative beam breakup for the various breakup modes is essential in order to determine the external loading necessary for its suppression. The principle of the measurement[9] depends on the fact that for currents I smaller than I_S the ratio P_b/P_s is proportional to I but independent of the energy W stored in the breakup mode in the structure. The starting current I_S is defined by the condition $P_b/P_s = 1$.

Experimentally, one excites the breakup mode by means of an external generator, operating the structure under acceleration conditions at the same time. Due to the energy exchange between particles and field both $W(I)$ and $Q_L(I)$ for $I \neq 0$ are different from their values $W(0)$ and $Q_L(0)$ for $I = 0$. Now one can show from power conservation that $P_b/P_s = 1 - Q_L(0)/Q_L(I)$. In addition we have $\omega W(I) = 4P_i Q_L^2(I)/Q_{ext}$, where P_i and Q_{ext} are the incident power and the external Q-value of the rf input probe. Thus, if P_i is held constant, we obtain

$$P_b/P_s = 1 - \sqrt{W(0)/W(I)} = 1 - \sqrt{P_{rad}(0)/P_{rad}(I)},$$

where P_{rad} is the power radiated out of a sensing probe. In our measurements we pulsed the beam current with a period of a few seconds and read P_{rad} from a spectrum analyzer, thereby getting rid of the signal at the accelerator mode frequency.

Experimental Results

In Tables I and II we summarize the $I_s Q_L$-values experimentally determined for the injector structures of the Stanford SCA. During these measurements the capture section and the pre-accelerator were operated at 3.3 and 2.5 MeV/m accelerating gradients respectively. The input and output energies were 0.11 MeV and 1.8 MeV for the capture section, and 1.8 MeV and 8 MeV for the pre-accelerator. A comparison between the measured $I_s Q_L$-values and their theoretical lower limits calculated previously, reveals that quantitatively the latter are useful only as guidelines. Qualitatively the theory predicts that the $I_s Q_L$-values in a given band are the smallest for modes which have space harmonics that travel only slightly slower than the particles. The results recorded in Tables I and II and the passbands in Figs. 2 and 3 agree in this respect.

Loading of Breakup Modes

The inherent Q-values in a superconducting structure are quite high, and thus to achieve large average beam currents care must be exercised that all relevant breakup modes are externally loaded. Our objective is to load all breakup modes so that their starting currents are 200 μA or larger. Loading of the TM_{01}-modes which can lead to longitudinal beam breakup is straightforward. If the rf input probe is located in the cell adjacent to the center cell of the structure, as shown in Fig. 1, the Q_{ext}-values for the neighbor modes will be of the same order of magnitude as that for the accelerator mode. These neighbor modes are the ones most apt to cause breakup in the TM_{01}-band. The resulting Q_{ext}-values for the neighbor modes, given in Tables I and II, indicate that the starting current for longitudinal beam breakup exceeds 800 μA.

Loading of the HEM_{11}-modes which can lead to transverse beam breakup is more complex. First each HEM_{11}-mode has two polarizations, and thus two probes located about 90° apart in the azimuthal direction must be provided to ensure that both polarizations are externally loaded. In addition, due to the complexity of the multiperiodic structure, there are four HEM_{11}-modes that must be separately loaded. If these four modes (in the pre-accelerator the 1.598 GHz, 1.741 GHz, 1.823 GHz, and 1.865 GHz modes) are properly loaded, then all other modes are also properly loaded.

The main problem in loading down the HEM_{11}-modes is that of achieving high selectivity, since one wants to load down the transverse breakup modes without coupling appreciable power out of the accelerator mode. The transverse mode at 1.598 GHz is the simplest to load in this respect, since it belongs to the TE_{11}-like branch of the HEM_{11}-band and thus exhibits strong radial electric field components E_r at the outer circumference of the structure. The selectivity of a probe coupling to the E_r fields of the 1.598 GHz mode is greater than 10^5. In the pre-accelerator for a starting current of 200 μA a loading of Q_{ext} (1.598 GHz) = 1.3 x 10^8 is necessary and for a typical energy gradient of 3.3 MeV/m the 1.3 GHz power coupled out of a single probe is less than one milliwatt. There would be little problem in increasing the starting current for this mode to one milliamp. The locations of the E_r probes in the injector structures are shown in Fig. 1, and the loading of the other modes in the TE_{11}-branch are given in Tables I and II.

The transverse mode at 1.741 GHz is the most difficult to load. This mode belongs to the TM_{11}-like branch of the HEM_{11}-band and thus its fields at the outer circumference of the structure in the center of the cells are similar to those of the accelerator mode. Furthermore, as mentioned previously, the 1.741 GHz mode is localized in the five long cells of each sub-structure. The 1.741 GHz modes therefore must be loaded down separately in each substructure by magnetic loop probes coupling to H_θ and the selectivity is unity. In the pre-accelerator for a starting current of 200 μA one needs Q_{ext} (1.741 GHz) = 2.8 x 10^8 and for a typical energy gradient of 3.3 MeV/m the 1.3 GHz power coupled out of a single probe is about 40 watts. Although this power is small compared to the rf input power, it is too large to be dissipated at helium temperature. There are two solutions to this problem. One can either terminate the probe at room temperature, or one can build a band-stop filter to reject the 1.3 GHz power. A suitable band-stop filter is described in the next section. The locations of the H_θ probes in the injector structures are shown in Fig. 1.

In the pre-accelerator the mode at 1.865 GHz which also belongs to the TM_{11}-like branch can be loaded by coupling to the H_z-component of its cutoff mode at the circumference of the beam pipe.

The TM_{11}-like structure mode couples to a TE_{11}-cut-off mode which has strong axial magnetic field components H_z at the outer circumference. The accelerator mode on the other hand, couples to the TM_{01}-cutoff mode which has no H_z components at all. Experiments show that for the 1.865 GHz mode a selectivity of about 500 can be achieved by this method of loading. The location of the H_z probes in the injector structures are shown in Fig. 1, and the loading of other TM_{11}-like modes by these probes are given in Tables I and II.

Bead measurements show that the 1.823 GHz mode which belongs to the TM_{11}-like branch of the pre-accelerator has very small field amplitudes in the long cells of each sub-structure and in the beam pipes, but has strong fields in the three short cells between sub-structures. By locating the loading probes, as shown in Fig. 1, in a cell in which two sub-structures are flanged together one can achieve sufficient loading. By design the field of the accelerator mode has a zero in these cells. Therefore, the selectivity will also be good, although the 1.823 GHz mode must be loaded down by magnetic loop probes coupling to H_θ. For a starting current of 200 μA , the necessary loading is Q_{ext} (1.823 GHz) = 8.5 x 10^7 , as shown in Table II.

In order to house the probes loading the HEM_{11}-modes coupling channels, constructed of niobium, are electron beam welded into the structures at the proper locations. The probes, also constructed of niobium, are flanged to these channels. The end of the center conductor in an E_r-probe will be 3 mm outside the cavity, whereas the loops in an H_θ probe will be 4 mm outside. Estimates show that the 1.3 GHz power dissipated in all probes is negligible compared to the power losses in the walls of the structure, and that heating of the probes beyond the transition temperature of niobium will certainly not occur.

Description of a Band-Stop Filter

The purpose of the band-stop filter[18] is to reject the power coupled out of the accelerator mode by a loading probe without affecting the coupling at the frequencies of the breakup modes between 1.5 and 1.9 GHz. This can be achieved by shunting the output of the loop probes with a resonant circuit in the form of a shorted coaxial line, $\lambda/2$ in length, λ being the wavelength corresponding to the accelerator mode frequency of 1.3 GHz. The design of the filter is illustrated in Fig. 4.

The width of the stopband can be chosen within some limits by the characteristic impedance of the resonant line. An impedance of 28 Ω was found to be optimal. The position of the shunt relative to the coupling loops is important and has to be approximately $\lambda/4$. Under this condition the wave travelling into the filter is reduced by a factor of 2 in the ideal lossless case compared to a wave excited by a loop probe with no filter. This

increases the attenuation of the filter by 6 dB and reduces the power dissipated in it.

An impedance transformer between the shunt and the loop increases the coupling for the break-up modes. The length of this transformer is one quarter wavelength at approximately 1.7 GHz and its characteristic impedance is 28 Ω . The 50 Ω output line connected to the shunt is thus transformed to a low impedance at the loop, which increases the loading by 5 dB . The shunt at these higher frequencies has changed to high impedance and does not affect the wave propagation much.

The performance of a brass test model is shown in Fig. 4. The maximum attenuation is 46 dB which indicates a Q of approximately 300 for the resonant stub. With this Q the losses in the filter are about 1 watt for 100 watts coupled power. Since this power would be dissipated in the liquid helium it was decided to make the filter superconducting and build it out of niobium. This will reduce the losses and increase the maximum attenuation at resonance considerably, although it will hardly change the attenuation at points $\pm$ 5 MHz or further away from resonance. The niobium version of this filter is being built but no results are available at this time.

Conclusion

The experiments with the superconducting injector system represent an important step in the development of the superconducting accelerator. It has been demonstrated that a beam intensity of 100 μA with a duty factor 1 can be achieved.

Acknowledgements

References

1. R. H. Helm, G. A. Loew, "Beam Breakup" in Linear Accelerators (P. M. Lapostolle, A. L. Septier, editors, North Holland Publ. Co. (1970).

2. P. B. Wilson, "Theory and Design of Superconducting Electron Accelerators", ibid.

3. A. Citron, H. Schopper, "Superconducting Proton Linear Accelerators and Particle Separators", ibid.

4. M. S. McAshan, H. A. Schwettman, L. Suelzle, J. P. Turneaure, HEPL-665 (1972), High Energy Physics Laboratory, Stanford University.

5. W. K. H. Panofsky, M. Bander, Rev. Sci. Instr. 39-2, 206 (1968).

6. R. H. Helm, SLAC-TN-67-6, Stanford Linear Accelerator Center, Stanford University and HEPL-TN-67-3, High Energy Physics Laboratory, Stanford University (1967).

7. P. B. Wilson, HEPL-TN-67-8, High Energy Physics Laboratory, Stanford University (1967).

8. P. B. Wilson, HEPL-297 (1963), HEPL-TN-67-2 (1962), HEPL TN-67-6 (1967), High Energy Physics Laboratory, Stanford University.

9. K. Mittag, M. Kuntze, F. Heller, J. E. Vetter, Nucl. Instr. Meth. 76, 245 (1969).

10. K. Mittag, Ext. Report 3/69-29 (1969) Kernforschungszentrum, Karlsruhe, Germany.

11. F. Heller, M. Kuntze, K. Mittag and J. Vetter, Ext. Report 3/69-11 (1969), Kernforschungszentrum, Karlsruhe, Germany.

12. F. Heller, Ext. Report. 3/71-6 (1971), Kernforschungszentrum, Karlsruhe, Germany.

13. K. Mittag, HEPL TN-72-3 (1972), High Energy Physics Laboratory, Stanford University.

14. B. W. Montague, "Radiofrequency Separators" in Linear Accelerators, (P. M. Lapostolle and A. L. Septier, editors) North Holland Publ. Co. (1970).

15. W. Bauer and H. Hahn, Part. Acc. 3 (1972), to be published.

16. Y. Garault, "Hybrid EH Guided Waves", in Advances in Microwaves Vol. 5 (L. Young, editor), Academic Press (1970).

17. G. Saxon, T. R. Jarvis and I. White, Proc. IEEE 10, 1365 (1963).

18. G. L. Matthaei, L. Young and E. M. T. Jones, "Microwave Filters, Impedance Matching Networks, and Coupling Structures", McGraw Hill (1964).

TABLE I

BEAM BREAKUP PROPERTIES OF THE CAPTURE SECTION

N^+	f(GHz)	$I_S Q_L (10^4 A)$	Probe[‡]	$Q_{ext}(10^7)$	Band
1	1.2497	-	rf in	0.9	TM_{01}
2	1.2565	-	"	1.6	"
3	1.2631	< 0	"	45	"
4	1.2790	19	"	0.6	"
5	1.2876	11	"	1.3	"
6	1.2975	1.7	"	2	"
7	1.3000	-	"	1	"
1	1.4693	46	E_r	100	TE_{11}
2	1.4980	17	"	50	"
3	1.5406	4.5	"	5	"
4	1.5974	2.6	"	13	"
5	1.6602	< 0	"	-	"
1	1.9056	25	H_z	120	TM_{11}
2	1.8952	12	"	15	"
3	1.8765	3.7	"	12	"
4	1.8635	< 0	"	12	"
5	1.8327	< 0	E_r, H_z	60, 60	"
6	1.7418	93	H_θ	300	"
7	1.7875	< 0	H_θ	-	"

+ mode number

‡ Probe which loads mode down to Q_{ext}; rf in, H_θ, H_z, E_r label both loading probes and fields to which probes couple (see Fig. 1).

TABLE II

BEAM BREAKUP PROPERTIES OF THE PRE-ACCELERATOR

N^+	f(GHz)	$I_S Q_L (10^4 A)$	Probe‡	$Q_{ext}(10^7)$	Band
1	1.2493	-	rf in	-	TM_{01}
2	1.2495	-	"	-	"
3	1.2496	-	"	-	"
4	1.2557	-	"	-	"
5	1.2560	-	"	-	"
6	1.2563	-	"	-	"
7	1.2621	-	"	-	"
8	1.2626	-	"	-	"
9	1.2629	-	"	-	"
10	1.2759	-	"	-	"
11	1.2773	-	"	-	"
12	1.2788	-	"	-	"
13	1.2821	-	"	-	"
14	1.2846	-	"	-	"
15	1.2875	> 32	"	1	"
16	1.2894	> 9.6	"	2	"
17	1.2912	> 16	"	0.8	"
18	1.2975	< 0	"	2	"
19	1.2981	> 14	"	3.5	"
20	1.2992	< 0	"	2	"
21	1.3000	-	"	1	"
22	1.3012	18	"	8	"
23	1.3017	-	"	0.9	"
3	1.5416 (G)	> 31	$E_r(G)$	5	TE_{11}
3	1.5407 (D)	> 21	$E_r(D)$	5	"
3	1.5398 (A)	> 23	$E_r(A)$	5	"
4	1.5982 (G)	2.6	$E_r(G)$	13	"
4	1.5971 (D)	3.0	$E_r(D)$	13	"
4	1.5965 (A)	4.4	$E_r(A)$	13	"
1	1.9073	-	H_z	1300	TM_{11}
2	1.9063	-	"	250	"
3	1.9051	-	"	150	"
4	1.9004	22	"	100	"
5	1.8971	-	"	34	"
6	1.8945	< 0	"	90	"
7	1.8865	-	"	60	"
8	1.8812	-	"	50	"
9	1.8751	30	"	29	"
10	1.8701	-	"	14	"
11	1.8654	3.7	"	18	"
12	1.8628	< 0	"	29	"
13	1.8375	< 0	"	420	"
14	1.8346	< 0	"	230	"
15	1.8326	6.9	$E_r(A+G)$	35	"
16	1.8245	< 0	$H_\theta(D,S)$	-	"
17	1.8229	1.7	$H_\theta(D,S)$	8.5	"
18	1.7417 (G)	5.6	$H_\theta(G)$	28	"
19	1.7412 (D)	12	$H_\theta(D,L)$	28	"
20	1.7405 (A)	-	$H_\theta(A)$	28	"
21	1.7882 (G)	< 0	$H_\theta(G)$	-	"
22	1.7880 (D)	< 0	$H_\theta(D,L)$	-	"
23	1.7874 (A)	< 0	$H_\theta(A)$	-	"

+ mode number

‡ Probe which loads mode down to Q_{ext}; rf in, H_θ, H_z, E_r label both loading probes and fields to which probes couple; A, D, G label sub-sections in pre-accelerator; L, S refer to long, short cells (See Fig. 1).
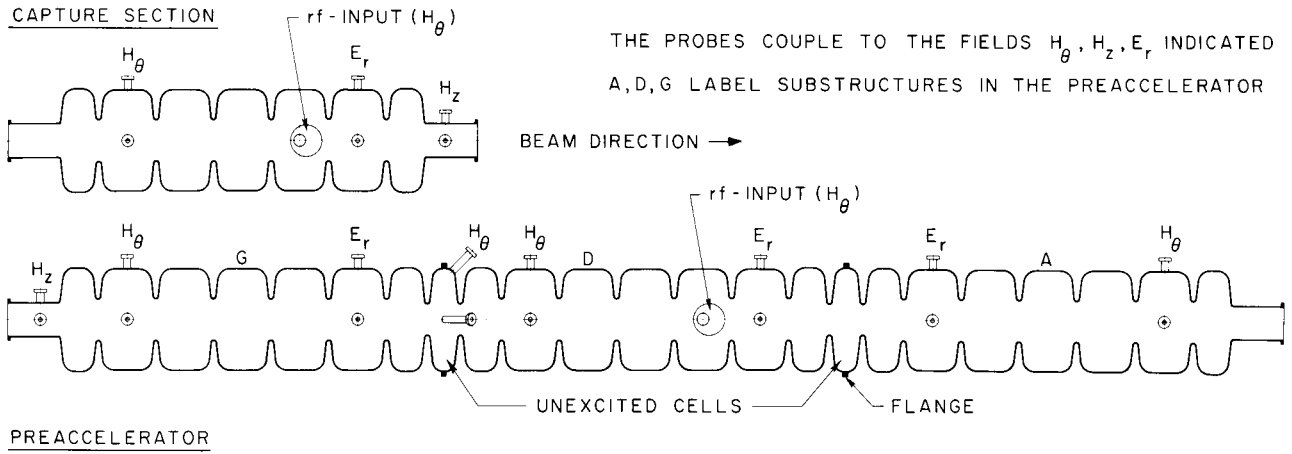
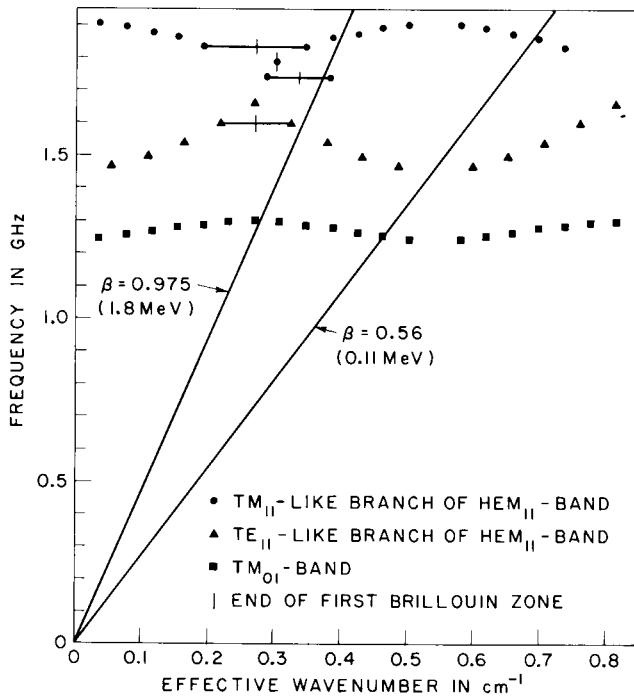Fig. 1.   Schematic of the Cryogenic Injector.
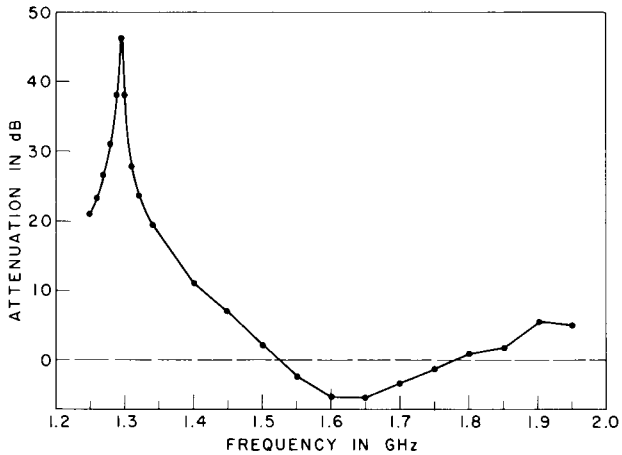

Fig. 2.   Lowest Passbands of the Capture Section.

Fig. 3.   Passbands of the Pre-accelerator.

Fig. 5.   Reduction of Output Power From Loop Probe
          by Means of a Band-stop Filter.
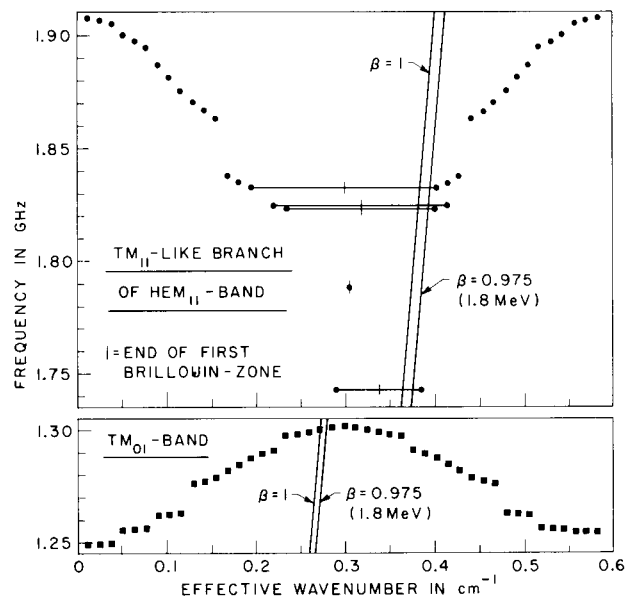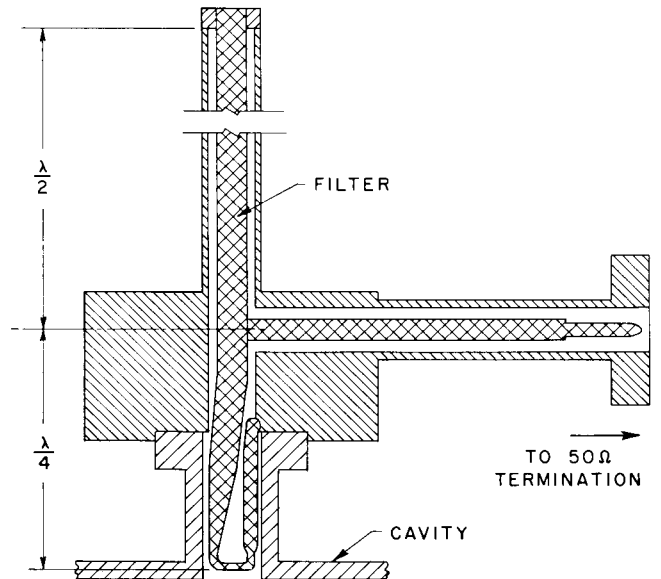

Fig. 4.   Schematic of Band-stop Filter.

DISCUSSION

James E. Leiss, NBS: You say that you achieved a threshold of 100 µamp. Could you clarify that? You mean 100 µamp for what length accelerator at what gradient?

Mittag: It is for a gradient of 3.3 MV/m and for the two structures of the cryogenic injector, but there is essentially no problem to load down the breakup modes for the subsequent structures by the same method.

Leiss: You talk about the multi-section blowup as opposed to the single-section blowup. If you provided the same techniques, could you say what kind of threshold you might expect on a longer accelerator?

Mittag: You mean the breakup that you have in a normally conducting accelerator like SLAC for instance. No, this is quite a different problem. The reason for this is that this breakup is "resonant breakup." The process works by exciting the breakup mode resonantly by the beam. Because of our high Q-values, the scattering and resonance frequencies in sequential structures for the same mode was quite large, of the order of 10-100 kHz. This is much larger than the bandwidths, and because of this, resonant beam breakup is no longer governed by the Q-value, as it is in a normally conducting accelerator, but by the average separation of frequencies in sequential structures. We made some estimates about this and found that the e-folding factor which you generally calculate for a normally conducting machine would be of the order of 4. At SLAC, one observed cumulative beam breakup with an e-folding factor of about 15, so we do not expect any problems.

Kenneth Whitham, Applied Radiation Corp.: How did you probe and identify the breakup fields? What techniques did you use?

Mittag: We mainly used bead measurements, and resonant frequency measurements.

Whitham: On axis?

Mittag: On axis and in some cases at the outer circumference of the structure where your loading probe is located.

Gregory A. Loew, SLAC: Could you write down a few of the significant Q-values before and after the loading so we have an idea of what you did? You gave some numbers like 10^5 but I was not able to follow the various modes. Could you just give a few examples of what you were able to do?

Mittag: If you do not do anything against loading, the Q-value for the breakup mode may be as high as 10^{10}. In order to suppress beam breakup, we have to load some of these modes down to 10^7 and others maybe only to 10^8, but the lowest value we have to get is 10^7.

Loew: Do you think that you will continue to do the same thing in the next sections; or will you do something different or less drastic in the number of probes?

Mittag: The number of probes will decrease the further you go along the accelerator, because the increase in energy makes the breakup more improbable; but we will have to provide some probes in the first few 6m sections also.

Loew: Is the 100 µsec for an infinite pulse length?

Mittag: Yes, a duty factor of one.

Loew: How fast does it go after that?

Mittag: It depends on how much you run the current above threshold. If you are very near to threshold, it may take as long as 10 sec or so before you get breakup. If you are much higher than threshold, let us say 20% higher, then the breakup is nearly instantaneous ($\sim$1/sec). That may be a time that corresponds to the Q-value of the breakup mode.

Loew: Did you actually plot a curve and compare it with theory in some way?

Mittag: No.

D. Schulze, Karlsruhe: (Question for L. Suelzle) In one of your earlier papers, you mentioned that the beam could turn on with a step function without significant breakdown in field because of fast amplitude control. Will that be the normal procedure due to present knowledge?

Suelzle: For CW operation, we were not too concerned about the sudden turn-on of the beam provided that when the beam was turned on the energy did not drop drastically. We picked a feedback response time that would allow us to turn on the beam to 100% value and have a drop of approximately one part in 2000. If the field was not servo locked, the field would start to decay at a rate determined by the beam current and stored energy. At some point, the feedback loop finds the field was dropping and then it starts to come back up. We chose what we thought would be a reasonable feedback response time for a gain bandwidth of approximately 10 kHz. This gives us a response time of about 16 µsec based on a very simple model. In 16 µsec it drops like one part in 2000 if I recall the numbers properly. We thought that this was adequate. If you are worried about it, e.g., if you want to use pulse operation and have short pulses, you would either need to improve the response time, or do as they do at Los Alamos, provide some presignal telling the system to turn on ahead of time, i.e., telling it that the beam is coming.